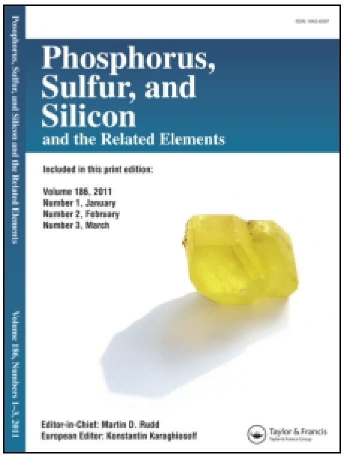

Phosphorus, Sulfur, and Silicon and the Related Elements
Publication details, including instructions for authors and subscription information:
http://www.informaworld.com/smpp/title~content=t713618290

Configurational Properties of N,N'-Dimethyl-1,3-Diazacyclohexane and Its Analogues Containing P and As Atoms: A Hybrid-DFT Study and NBO Interpretation

Alireza Zinlynezhad[a]; Davood Nori-Shargh[b]; Neda Najma[c]; Hooriye Yahyaei[d]
[a] Chemistry Department, Islamic Azad University, Anar Branch, Anar, Iran [b] Chemistry Department, Islamic Azad University, Poonak, Tehran, Iran [c] Chemistry Department, Science Faculty, Islamic Azad University, Arak Branch, Arak, Iran [d] Chemistry Department, Islamic Azad University, Zanjan Branch, Zanjan, Iran

To cite this Article Zinlynezhad, Alireza , Nori-Shargh, Davood , Najma, Neda and Yahyaei, Hooriye(2011) 'Configurational Properties of N,N'-Dimethyl-1,3-Diazacyclohexane and Its Analogues Containing P and As Atoms: A Hybrid-DFT Study and NBO Interpretation', Phosphorus, Sulfur, and Silicon and the Related Elements, 186: 1, 44 — 57
To link to this Article: DOI: 10.1080/10426501003776954
URL: http://dx.doi.org/10.1080/10426501003776954

Phosphorus, Sulfur, and Silicon, 186:44–57, 2011
Copyright © Taylor & Francis Group, LLC
ISSN: 1042-6507 print / 1563-5325 online
DOI: 10.1080/10426501003776954

CONFIGURATIONAL PROPERTIES OF N,N′-DIMETHYL-1,3-DIAZACYCLOHEXANE AND ITS ANALOGUES CONTAINING P AND As ATOMS: A HYBRID-DFT STUDY AND NBO INTERPRETATION

Alireza Zinlynezhad,[1] Davood Nori-Shargh,[2] Neda Najma,[3] and Hooriye Yahyaei[4]

[1]*Chemistry Department, Islamic Azad University, Anar Branch, Anar, Iran*
[2]*Chemistry Department, Islamic Azad University, Science and Research Branch, Hesarak, Poonak, Tehran, Iran*
[3]*Chemistry Department, Islamic Azad University, Science Faculty, Arak Branch, Arak, Iran*
[4]*Chemistry Department, Islamic Azad University, Zanjan Branch, Zanjan, Iran*

GRAPHICAL ABSTRACT

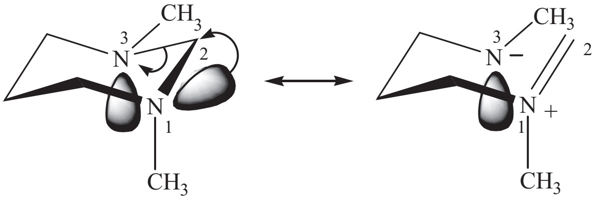

Abstract *The configurational properties of N,N′-dimethyl-1,3-diazacyclohexane (**1**), N,N′-dimethyl-1,3-diphosphacyclohexane (**2**), and N,N′-dimethyl-1,3-diarsenacyclohexane (**3**) have been analyzed by means of hybrid density functional theory (B3LYP/6-311+G**)–based method and NBO interpretation. The NBO analysis of donor–acceptor (bond—antibond) interactions revealed that the calculated generalized anomeric effects (GAE) between the equatorial* ee-ae, ea-aa, *and* ee-aa *configurations decrease from compound **1** to compound **3**. Contrary to the decrease of the GAE values for* ee-ea *configurations, the* ea *configuration stability increases from compound **1** to compound **3**. This could be explained reasonably by the decrease of the nonbonded steric repulsions (by lengthening of the C—M bond lengths increase from compound **1** to compound **3**) between the* ee, ea, *and aa configurations from compound **1** to compound **3**. The correlations between the GAE, Wiberg bond indexes (WBI), natural bond orders (NBOs), dipole moments, orbital integrals, structural parameters, and Gibbs free energy difference* (G_{ee}–$G_{ea,}$ G_{ea}–G_{aa} G_{ee}–G_{aa}) *values (i.e.,* $\Delta G_{ee\text{-}ea}$, $\Delta G_{ea\text{-}aa}$, $\Delta G_{ee\text{-}aa}$) *values between the* ee, ea, *and* aa *configurations of compounds **1–3** have investigated.*

Keywords DFT; N,N′-dimethyl-1,3-diazacyclohexane; generalized anomeric effects; molecular modeling; NBO

Received 11 February 2010; accepted 15 March 2010.

Address correspondence to Davood Nori-Shargh, Chemistry Department, Islamic Azad University, Science and Research Branch, Hesarak, Poonak, Tehran, Iran. E-mail: nori_ir@yahoo.com

INTRODUCTION

Saturated heterocyclic compounds comprise a large segment of chemical compounds and are quite widespread in nature (e.g., in alkaloids, carbohydrates, and plant growth regulators, among other compounds). Therefore knowledge about conformational properties of this kind of compound should be of very general interest.

It is well known that the stereoelectronic interactions play an important role on the conformational properties of heterocyclic compounds.[1,2] The striking observation that a substantial proportion of N,N′-dimethyl-1,3-diazacyclohexane (1) exists in equatorioal-axial (*ea*) configuration with one methyl group axial was described by Riddell and Williams,[3] Jones et al.,[4] and Elilel et al.[5,6] It seems that the orientations of methyl groups in compound **1** could depend upon the relative magnitude of nonbonded, dipolar, and stereoelectronic interactions. In this regard, there is a substantial disfavoring factor in *ee* configuration in which unshared electron pairs are parallel (the "rabbit-ear effect").[6,7]

There are published theoretical data on the structure and the anomeric effect (*AE*) of methandiamine [$CH_2(NH_2)_2$],[8–10] but no experimental data are available. Ab initio MO calculations,[11,12] gas electron diffraction (GED), IR, and He(I) photoelectron spectroscopy have been performed to investigate the impact of the *AE* on the structural parameters of methylenebis(phosphane) [$CH_2(PH_2)_2$].[12] The structural properties of methylenediarsine [$CH_2(AsH_2)_2$] have been investigated by means of ab initio and NBO analysis.[9]

It should be noted that the generalized anomeric effect (GAE) associated with electronic delocalizations is in favor of the axial conformation of a six-membered saturated ring, in opposition to the steric effect, which normally leads to a preference for the equatorial conformation. There is a stereoelectronic preference for conformations in which the best donor lone pair is antiperiplanar to the best acceptor bond. Based on this argument, we could stress that the GAE must be considered as the difference between the sum of the equatorial and axial delocalization energies:

$$\text{GAE} = \sum(GAE_{\text{eq}}) - \sum(GAE_{\text{ax}}) \qquad (1)$$

There is sufficient published experimental information about the configurational properties of compound **1**;[3,7] however, there is no published experimental or quantitatively theoretical data about the donor–acceptor delocalization effects on the conformational properties of compounds **1–3**. In this article, the impacts of the stereoelectronic interactions associated with GAE, bond orders, dipole moments, orbital integrals, structural parameters, and configurational and structural properties of compounds **1–3** are investigated computationally using the hybrid-DFT method (B3LYP/6-311+G**) (see Scheme 1).[13–18] Also, the energy differences between the various configurations of compounds **1–3** have been

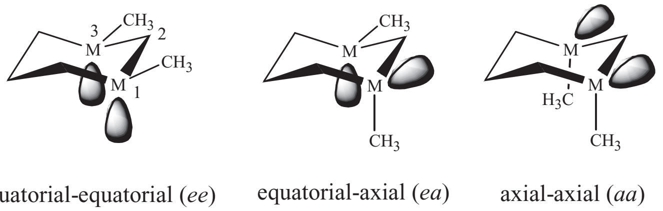

equatorial-equatorial (*ee*) equatorial-axial (*ea*) axial-axial (*aa*)

Scheme 1 Schematic representation of configurations of compounds **1–3**. [Numbering used for compounds **1–3** (**1**: M=N, **2**: M=P, **3**: M=As)].

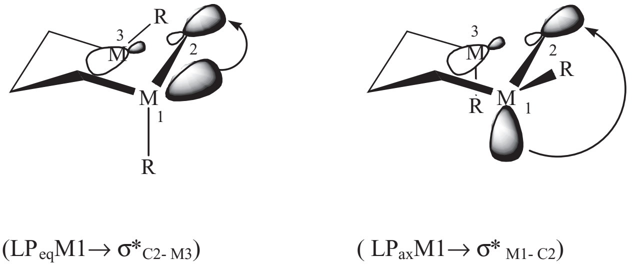

Figure 1 Schematic representation of hyperconjugation between bonding and antibonding orbitals ($LP_{eq}M1 \rightarrow \sigma^*_{C2\text{-}M3}$ and $LP_{ax}M1 \rightarrow \sigma^*_{M1\text{-}C2}$).

compared with those in 1,3-dimethylcyclohexane (4). This comparison gives a clear feature for the impacts of the stereoelectronic effects, dipole–dipole interactions, and nonbonded steric repulsions on the configurational properties of compounds **1–3**.

The successful application of density functional theory (DFT)–based methods has broadened the applicability of the computational methods and now represents an interesting approach for determining activation barrier and molecular energies.[13–18] The B3LYP method combines Becke's three-parameter exchange function with the correlation function of Lee et al.[15] The NBO analysis is a sufficient approach to investigate the effect of the stereoelctronic interactions on the stability, reactivity, and dynamic behaviors of chemical compounds.[19–28]

Also, the stabilization energies (E_2) associated with $LP_{eq}M1 \rightarrow \sigma^*_{C2\text{-}M3}$ and $LP_{ax}M1 \rightarrow \sigma^*_{C2\text{-}M3}$ delocalizations (see Figures 1 and 2) and their influences on the configurational properties of compounds **1–6** were quantitatively investigated by natural bond orbital (NBO) analysis.[29] It should be noted that the $LP \rightarrow \sigma^*$ stabilization energies are proportional to $S^2/\Delta E$, where S is the orbital overlap and ΔE is the energy differences between the LP and σ^* orbitals:[30]

$$\text{Stabilization or resonance energy } \alpha \ (S^2/\Delta E)$$

In addition, the stabilization energy (E_2) associated with $i \rightarrow j$ delocalization is explicitly estimated by the following equation:

$$E_2 = q_i \frac{F^2(i, j)}{\varepsilon_j - \varepsilon_i}$$

where q_i is the ith donor orbital occupancy, ε_i and ε_j are diagonal elements (orbital energies), and F(i,j) off-diagonal elements, respectively, associated with the NBO Fock matrix. Therefore, there is a direct relationship between F(i,j) off-diagonal elements and the orbital overlap (S_{ij}).

COMPUTATIONAL DETAILS

Calculations were carried out using the hybrid density functional theory (B3LYP/6-311+G**//B3LYP/6-311+G**)–based method with the Gaussian 98 package of programs.[13] Since the main purpose of the present work was to evaluate the impacts of the GAE and dipole moments on the structural and configurational properties of compounds **1–3**, the energy minimization was carried out only for the *ee*, *ea*, and *aa* configurations

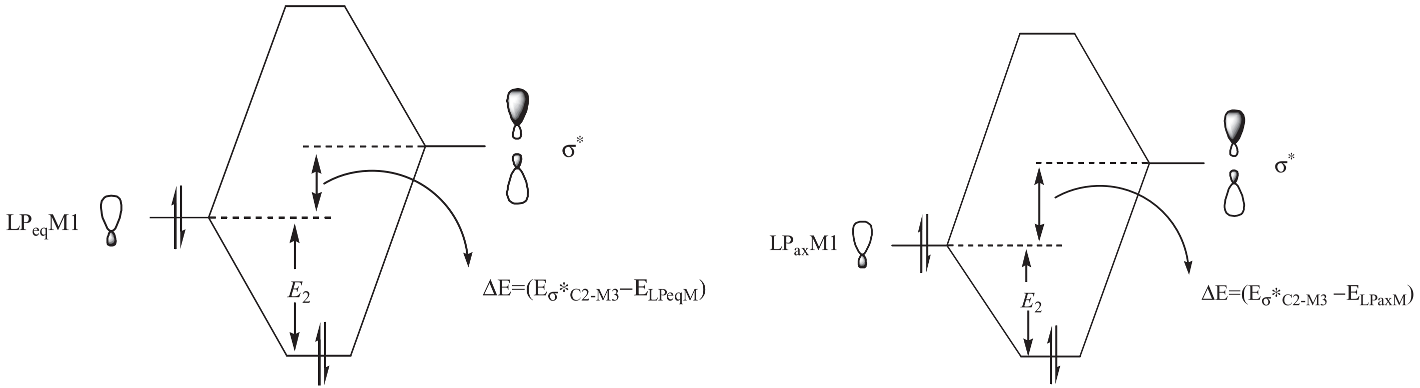

Figure 2 Schematic representation of stabilization energy (E_2) associated with the electron delocalization from donor (nonbonding) to acceptor (antibonding) orbitals.

of the heterocyclic rings. The comparison of the energy differences between the various configurations of compounds **1–3** with those in 1,3-dimethylcyclohexane (**4**) gives a clear feature for the impacts of the stereoelectronic effects on the configurational properties of compounds **1–3**.

An NBO analysis was then performed for the axial and equatorial conformations of compounds **1–3** by the NBO 5.G program contained in the PC-GAMESS interface.[27]

The bonding and antibonding orbital occupancies in the various configurations of compounds **1**–**3**, and also the stabilization energies associated with $LP_{eq}M1 \rightarrow \sigma^*_{C2\text{-}M3}$ and $LP_{ax}M1 \rightarrow \sigma^*_{C2\text{-}M3}$ electronic delocalizations, were calculated using NBO analysis. The stabilizing orbital interactions are inversely proportional to the energy difference between the interacting orbitals; therefore, the strongest stabilizing interactions will take place between the most effective donors and the most effective acceptors (see Figures 1 and 2).

The thermodynamic functions (all corrected for the zero-point energy), i.e., enthalpy H (sum of the electronic and the thermal enthalpy), Gibbs free energy G (sum of the electronic and thermal free energy), and entropy S, were calculated according to the following relation: $E = E_o + E_{vib} + E_{rot} + E_{trans}$, $H = E + RT$, $G = H - TS$, as defined in the output of the frequency calculation in the Gaussian 98 manual. Finally, using the corresponding calculated thermodynamic data for ground and transition states, ΔG, ΔH, and ΔS were also determined.

RESULTS AND DISCUSSION

Configurational Preferences

The Gibbs free energy, enthalpy, and entropy for the *ee*, *ea*, and *aa* configurations of compounds **1–4**, as calculated by the density functional theory (B3LYP/6-311+G** level of theory), are given in Table 1. Based on the calculated Gibbs free energy values, the *ee* configurations of compounds **1–3** are more stable than their *ea* and *aa* configurations. The calculated $\Delta G_{ee\text{-}ea}$ values for compounds **1–3** are 0.75, 0.45, and 0.40 kcal mol^{-1}, respectively. The calculated ΔG values between the *ee* and *ea* configurations of compound **1** (i.e., 0.75 kcal mol^{-1}) are in accordance with the published experimental data (i.e., 0.13 kcal mol^{-1}).[3–7] It should be remembered that our calculations were done for single molecules, and it is apparent that solvation plays a significant role in the conformational preferences of these compounds. Also, the *aa* configurations of compounds **1–3** are less stable than the corresponding *ee* configurations by 4.53, 3.82, and 2.59 kcal mol^{-1}, respectively. Based on the results obtained, the energy differences between the *ee-ea*, *ee-aa*, and *ea-aa* configurations decrease from compound **1** to compound **3**. It should be noted that the energy differences between the *ee-ea*, *ee-aa*, and *ea-aa* configurations of compounds **1–3** are smaller than those of compound **4** (see Table 1). This fact is as a result of the impact of the GAE on the various configurations of compounds **1–3**.

Generalized Anomeric Effects (GAE)

NBO analysis was used to investigate the electronic delocalizations because they are expected to have an impact on the bonding nature in the ground state structures (*ee*, *ea*, and *aa* configurations) of compounds **1–3**.

Table 1 B3LYP/6-311+G** calculated thermodynamic parameters [enthalpies, Gibbs free energies (in Hartree), and entropies (in cal mol^{-1} K^{-1})] for the *ee*, *ea*, and *aa* configurations of compounds **1–4**

Geometries	*H* (Hartree)	*S* (cal mol^{-1} K^{-1})	*G* (Hartree)	ΔH^a (Hartree)	ΔS^a (calmol^{-1} K^{-1})	ΔG^a (Hartree)	ΔG^c
1-*ee*	−346.436971	86.662	−346.478147	0.000000 (0.00)^b	0.000	0.000000 (0.00)^b	
1-*ea*	−346.435768	86.687	−346.476956	0.001203 (0.75)^b	0.025	0.001191 (0.75)^b	0.13^c
1-*aa*	−346.429398	87.394	−346.470922	0.007573 (4.75)^b	0.732	0.007225 (4.53)^b	
2-*ee*	−919.706523	98.165	−919.753165	0.000000 (0.00)^b	0.000	0.000000 (0.00)^b	
2-*ea*	−919.705853	98.051	−919.752440	0.00067 (0.42)^b	−0.114	0.000725 (0.45)^b	
2-*aa*	−919.700683	97.652	−919.747081	0.00584 (3.66)^b	−0.513	0.006084 (3.82)^b	
3-*ee*	−4708.705092	106.003	−4708.755458	0.000000 (0.00)^b	0.000	0.000000 (0.00)^b	
3-*ea*	−4708.704248	106.452	−4708.754827	0.000844 (0.53)^b	0.449	0.000631 (0.40)^b	
3-*aa*	−4708.700372	107.263	−4708.751336	0.00472 (2.96)^b	1.260	0.004122 (2.59)^b	
4-*ee*	−314.362031	88.246	−314.403960	0.000000 (0.00)^b	0.000	0.000000 (0.00)^b	
4-*ea*	−314.358246	87.815	−314.399969	0.003785 (2.38)^b	−0.431	0.003991 (2.50)^b	
4-*aa*	−314.352134	87.694	−314.393800	0.009897 (6.21)^b	−0.552	0.01016 (6.38)^b	

[a] Relative to the ground state.

[b] Numbers in parentheses are the corresponding thermodynamic functions values in kcal mol^{-1}.

[c] Experimental, see Ref. 7.

According to the NBO results, the *ee*, *ea*, and *aa* configurations of compounds **1–3** benefit from some donor–acceptor interactions. Based on the optimized ground state geometries, the NBO analysis of donor–acceptor (bond—antibond) interactions showed that the stabilization energy associated with $LP_{ax}M1 \rightarrow \sigma^*_{C2\text{-}M3}$ electronic delocalization for the *ee* configuration of compound **1** is 2.15 kcal mol^{-1}. Importantly, there is not this kind of the electronic delocalization for the *ea and aa* configurations of compound **1** and also for the *ee*, *ea*, and *aa* configurations of compounds **2** and **3**. In this regard, the stabilization energy associated with $LP_{eq}M1 \rightarrow \sigma^*_{C2\text{-}M3}$ electronic delocalization for the *ea* configurations of compounds **1–3** are 10.27, 4.16, and 3.01 kcal mol^{-1}, respectively. Also, the NBO analysis showed that the stabilization energy associated with $LP_{eq}M1 \rightarrow \sigma^*_{C2\text{-}M3}$ electronic delocalizations for the *aa* configurations of compounds **1–3** are 10.74, 5.63, and 3.936 kcal mol^{-1}, respectively (see Table 2). Effectively, the NBO analysis revealed that the stabilization energies associated with $LP_{eq}M1 \rightarrow \sigma^*_{C2\text{-}M3}$ electronic delocalizations decrease from the *ea* and *aa* configurations of compound **1** to compound **3**. Based on the results obtained, the sum of the stabilization energies associated with $LP_{eq}M1 \rightarrow \sigma^*_{C2\text{-}M3}$, $LP_{ax}M1 \rightarrow \sigma^*_{C2\text{-}M3}$, $LP_{eq}M3 \rightarrow \sigma^*_{C2-M1}$, and $LP_{ax}M3 \rightarrow \sigma^*_{C2-M1}$ electronic delocalizations increase from the *ee* configurations of compounds **1–3** to their corresponding *aa* configurations. The NBO results showed that the sum of the stabilization energies associated with $LPM1 \rightarrow \sigma^*_{C2\text{-}M3}$ and

Table 2 NBO calculated stabilization energies (E_2), off-diagonal elements (F_{ij}), generalized anomeric effects (GAE), dipole moments [μ (Debye)], Wiberg bond index matrixes (WBI) in the natural atomic orbitals (NAOs) basis, and natural bond orders (NBOs), based on the geometries calculated at the B3LYP/6-311+G** level of theory for the *ee*, *ea*, and *aa* configurations of compounds **1–3**

	1			**2**			**3**		
	aa	*ea*	*Ee*	*aa*	*ea*	*ee*	*aa*	*ea*	*ee*
Donor→acceptor									
$LP_{ax}M1 \rightarrow \sigma^*_{C2\text{-}M3}$	—	—	2.15(0.034)[a]	—	—	—	—	—	—
$LP_{eq}M1 \rightarrow \sigma^*_{C2\text{-}M3}$	10.74(0.074)[a]	10.27(0.072)[a]	—	5.63(0.051)[a]	4.16(0.044)[a]	—	3.96 (0.044)[a]	3.01(0.038)[a]	—
$LP_{ax}M3 \rightarrow \sigma^*_{C2\text{-}M1}$	—	2.16(0.034)[a]	2.15(0.034)[a]	—	—	—	—	—	—
$LP_{eq}M3 \rightarrow \sigma^*_{C2\text{-}M1}$	10.74(0.074)[a]	—	—	5.63(0.051)[a]	—	—	3.96 (0.044)[a]	—	—
Σ	21.48	12.43	4.30	11.26	4.16	0.00	7.92	3.01	0.00
		−8.13			*−4.16*			*−3.01*	
GAE		*−9.05*			*−7.10*			*−4.91*	
		−17.18			*−11.26*			*−7.92*	
μ (Debye)	1.20	0.81	1.01	1.77	1.29	2.38	1.40	1.04	1.90
bond order (Wiberg Bond Index)	0.9720	0.9970	0.9791	0.9157	0.9233	0.9243	0.8993	0.9054	0.9090
M1-C2	0.9720	0.9463	0.9791	0.9157	0.9207	0.9243	0.8993	0.9048	0.9090
C2-M3		0.0507			0.0026			0.0006	
$\Delta(WBI_{M1\text{-}C2,\ C2\text{-}M3})$	1.0097	1.0132	1.0101	0.9883	1.0035	0.9983	0.9756	0.9954	0.9998
Bond order (Natural bond order)	1.0097	1.0091	1.0101	0.9883	0.9937	0.9983	0.9756	0.9940	0.9998
M1-C2		0.0041			0.0098			0.0014	
C2-M3									
$\Delta(NBO_{M1\text{-}C2,\ C2\text{-}M3})$									

[a] Numbers in parentheses are the off-diagonal element (F_{ij}) values.

LPM3$\rightarrow\sigma^*_{\mathrm{C2-M1}}$ electronic delocalizations for the *ee*, *ea*, and *aa* configurations decrease from compound **1** to compound **3** (see Table 2). Based on Equation (1), the calculated GAE associated with LPM1$\rightarrow\sigma^*_{\mathrm{C2\text{-}M3}}$ and LPM3$\rightarrow\sigma^*_{\mathrm{C2-M1}}$ electronic delocalizations for the *ee* and *ea* configurations of compounds **1–3** are −8.13, −4.16, and −3.01 kcal mol^{-1}, respectively. Further, the calculated GAE for the *ea* and *aa* configurations of compounds **1–3** are −9.05, −7.10, and −4.91 kcal mol^{-1}, respectively. Furthermore, the NBO results revealed that the calculated GAE for the *ee* and *aa* configurations of compounds **1–3** are −17.18, −11.26, and −7.92 kcal mol^{-1}, respectively (see Table 2). It can be expected that with the decrease of the GAE, the energy differences between the *ee*, *ea*, and *aa* configurations of compounds **1–3** could be increased, but it seems that other factors (such as nonbonded steric repulsions and dipole moments) have important impacts on the configurational properties on compounds **1–3**.

Orbital Occupancies

The NBO results showed that the LP$_{\mathrm{eq}}$M nonbonding orbital occupancies in the *ea* and *aa* configurations increase from compound **1** to compound **3**, but the corresponding $\sigma^*_{\mathrm{C2-N}}$ antibonding orbital occupancies decrease. The increase of the LP$_{\mathrm{eq}}$M nonbonding orbital occupancies and also the decrease of the $\sigma^*_{\mathrm{C2\text{-}M3}}$ antibonding orbital occupancies in the *ea* and *aa* configurations from compound **1** to compound **3** could be justified by the decrease of the LP$_{\mathrm{eq}}$M1$\rightarrow\sigma^*_{\mathrm{C2\text{-}M3}}$ and LP$_{\mathrm{eq}}$M3$\rightarrow\sigma^*_{\mathrm{C2-M1}}$ electronic delocalizations from the *ea* and *aa* configurations of compound **1** to compound **3** (see Table 3).

Overlap Matrix Elements and $\Delta(E_{\mathrm{acceptor\text{-}donor}})$

It has to be noted that the preferred geometry of many molecules can be viewed as the result of the maximization of an interaction between the best donor bonding or nonbonding orbitals and the best acceptor antibonding orbitals. The resonance energies associated with LP$\rightarrow\sigma^*$ electronic delocalization are proportional to $S^2/\Delta E$, where S is the overlap integral of two interacting orbitals and ΔE is the energy differences between the LP nonbonding and σ^* antibonding orbitals. In this regard, the stereoelectronic orbital interactions are anticipated to be more effective for *anti*, rather than *syn* or *gauche*, arrangement between the donor (LP) and acceptor (σ^*) orbitals, and the stabilization should increase as the antibonding orbital σ^* energy decreases and the nonbonding orbital LP energy increases.

Table 3 Calculated nonbonding and antibonding orbital occupancies for the *ee*, *ea*, and *aa* configurations of compounds **1–3**, using NBO analysis, based on the optimized structures by the B3LYP/6-311+G** level of theory

Occupancy	LP$_{\mathrm{ax}}$M$_1$	LP$_{\mathrm{eq}}$M$_1$	LP$_{\mathrm{ax}}$M$_3$	LP$_{\mathrm{eq}}$M$_3$	$\sigma^*_{\mathrm{C2\text{-}M1}}$	$\sigma^*_{\mathrm{C2\text{-}M3}}$
1-*ee*	1.87268	—	1.87268	—	0.02653	0.02653
1-*ea*	—	1.87261	1.87528	—	0.02675	0.04720
1-*aa*	—	1.86789	—	1.86790	0.04906	0.04907
2-*ee*	1.95338	—	1.95338	—	0.02112	0.02112
2-*ea*	—	1.94484	1.95163	—	0.02575	0.03320
2-*aa*	—	1.94055	—	1.94055	0.04167	0.04167
3-*ee*	1.97349	—	1.97348	—	0.01994	0.01994
3-*ea*	—	1.96331	1.97200	—	0.02512	0.03017
3-*aa*	—	1.96075	—	1.96075	0.03740	0.03740

Table 4 Calculated nonbonding and antibonding orbital energies for the *ee*, *ea*, and *aa* configurations of compounds **1–3**, using NBO analysis, based on the optimized structures by B3LYP/6-311+G** level of theory

Energy	$LP_{ax}M_1$	$LP_{eq}M_1$	$LP_{ax}M_3$	$LP_{eq}M_3$	$\sigma^*_{M1\text{-}C2}$	$\sigma^*_{C2\text{-}M3}$
1-*ee*	−0.26744	—	−0.26743	—	0.36394	0.36394
1-*ea*	—	−0.25648	−0.27094	—	0.37702	0.34755
1-*aa*	—	−0.25036	—	−0.25036	0.36096	0.36095
2-*ee*	−0.39495	—	−0.39495	—	0.19337	0.19337
2-*ea*	—	−0.38275	−0.39397	—	0.19537	0.19454
2-*aa*	—	−0.38075	—	−0.38077	0.19520	0.19521
3-*ee*	−0.49044	—	−0.49044	—	0.13475	0.13476
3-*ea*	—	−0.47818	−0.48934	—	0.13729	0.13611
3-*aa*	—	−0.47629	—	−0.47629	0.13713	0.13713

Based on the NBO results, the energy difference between donor (E_{LPeqM1}) and acceptor ($E_{\sigma^*C2\text{-}M3}$) orbitals [i.e., $\Delta(E_{\sigma^*C2\text{-}M3}–E_{LPeqM1})$] for the *ea* configurations decrease from compound **1** to compound **2** but increase from compound **2** to compound **3**. In this context, the $\Delta(E_{\sigma^*C2\text{-}M3}–E_{LPeqM1})$ values for the *ea* configurations of compounds **4–6** are 0.60403, 0.57729, and 0.61429 a.u., respectively (see Tables 4 and 5). Importantly, the observed trend for the variation of the calculated $\Delta(E_{\sigma^*C2\text{-}M3}–E_{LPeqM1})$ values in the *ea* configurations of compounds **1–3** is the same with those in their corresponding *aa* configurations.

The NBO analysis revealed that the calculated off-diagonal elements F_{ij} for $LP_{eq}M1 \rightarrow \sigma^*_{C2\text{-}M3}$ and $LP_{eq}M3 \rightarrow \sigma^*_{C2-M1}$ electronic delocalizations decrease from the *ea* and *aa* configurations of compound **1** to compound **3** (see Table 2). Based on the results obtained, the contribution of the *GAE* in the *ea* and *aa* configurations of compounds **1–3** and can be controlled by the off-diagonal [or orbital overlap (S)] factor. It should be noted that the decrease of F_{ij} [or the orbital overlap (S)] values could be justified by the increase of M atom radiuses from compound **1** to compound **3**.

Dipole Moments

Further, it is well known that there is a preference for the conformation with the smallest resultant dipole moment. Especially in the gas phase, it is generally found that

Table 5 Calculated nonbonding and antibonding orbital energy differences for the *ee*, *ea*, and *aa* configurations of compounds **1–3**, using NBO analysis, based on the structures optimized at the B3LYP/6-311+G** level of theory

Energy	$\Delta(E\sigma^*_{(C2\text{-}M3)}–E_{LPaxM1})$	$\Delta(E\sigma^*_{(C2\text{-}M3)}–E_{LPeqM1})$	$\Delta(E\sigma^*_{(M1\text{-}C2)}–E_{LPaxM3})$	$\Delta(E\sigma^*_{(M1\text{-}C2)}–E_{LPeqM3})$
1-*ee*	0.63138	—	0.63137	—
1-*ea*	—	0.60403	0.64796	—
1-*aa*	—	0.61131	—	0.61132
2-*ee*	0.58832	—	0.58832	—
2-*ea*	—	0.57729	0.58934	—
2-*aa*	—	0.57596	—	0.57597
3-*ee*	0.6252	—	0.62519	—
3-*ea*	—	0.61429	0.62663	—
3-*aa*	—	0.61342	—	0.61342

the conformation with the larger dipole moment has the larger electrostatic energy and therefore an increased overall energy.[31] Table 2 presents the calculated dipole moments for the *ee*, *ea*, and *aa* configurations of compounds **1–3**. The dipole moments for the *ea* configurations of compounds **1–3** are less than those of the *ee* and *aa* configurations (see Table 2). Consequently, the rationalization of the configuration preference solely in terms of dipole–dipole interactions fails to account quantitatively for the *ee* preferences in compounds **1–3**. The differences between the calculated dipole moments for the *ee* and *ea* configurations of compounds **1–3** are 0.2036, 1.0902, and 0.8663 Debye, respectively. These results indicate that *ea* configurations of compounds **2** and **3** benefit more from dipole–dipole interactions, compared to *ea* configuration of compound **1**. Since the GAE for the *ee–ea* configurations decrease from compound **1** to compound **3**, the variations of the differences of the dipole moments between the *ee-ea* configurations reasonably explain the decrease of the energy differences between the *ee* and *ea* configurations from compound **1** to compound **3**.

Bond Orders [Wiberg Bond Indexes (WBIs) and Natural Bond Orders (NBOs)]

The $LP_{eq}M1 \rightarrow \sigma^*_{C2\text{-}M3}$ and $LP_{eq}M3 \rightarrow \sigma^*_{C2-M1}$ electronic delocalizations affect the bond orders of M1-C2 and C2-M3 bonds. Based on the results obtained, the calculated bond orders [Wiberg bond index (WBI)] for C2-M3 bonds of the *ea* configurations are smaller than M1-C2 bonds (see Table 2). It should be noted that the differences between the calculated WBI of the M1-C2 and C2-M3 bonds in the *ea* configurations conformations decrease from compound **1** to compound **3**. Our NBO analysis revealed that the calculated $\Delta(WBI_{\text{anti-gauche},\ \text{M1-C2}})$ parameters for the *ea* configurations of compounds **1–3** are 0.0507, 0.0026, and 0.0006, respectively. The drastic increase of the calculated $\Delta(WBI_{\text{M1-C2}-\text{C2-M3}})$ parameters is in accordance with the decrease of the calculated *GAE* values from compound **1** to compound **3** (see Table 2).

In addition, the NBOs for the *ee*, *ea*, and *aa* configurations of compounds **1–3** have been calculated. The calculated NBOs for C2-M3 bonds of the *ea* configurations are smaller than M1-C2 bonds (see Table 2). This fact can be explained by the $LP_{eq}M1 \rightarrow \sigma^*_{C2\text{-}M3}$ electron delocalization. The calculated $\Delta(NBO_{\text{M1-C2, C2-M3}})$ parameters for the *ea* configurations of compounds **1–3** are 0.0041, 0.0098, and 0.0014, respectively. Obviously, based on the results obtained, the decrease of the calculated $\Delta(WBI_{\text{anti-gauche},\ \text{M1-C2}})$ values from the *ea* configuration of compound **1** to compound **3** can be reasonably explained by the decrease of their corresponding GAE values, compared to the calculated corresponding NBOs values (see Table 2).

Structural Parameters

Representative structural parameters for the *ee*, *ea*, and *aa* configurations of compounds **1–4**, as calculated by the B3LYP/6-311+G** level of theory, are shown in Table 6. Importantly, consideration of the structures of the *ea* configurations of compound **1** gave evidence that in the *ea* configurations of these compounds, the $\sigma_{\text{M1-C2}}$ bond lengths are significantly contracted compared to their $\sigma_{\text{C2-M3}}$ bonds. B3LYP/6-311+G** results show that the $\sigma_{\text{M1-C2}}$ and $\sigma_{\text{C2-M3}}$ bond lengths in the *ea* configurations of compound **1** are as follows: 1.448, 1.472 Å (see Table 6 and Scheme 2). This fact could be a result of the strong

Table 6 B3LYP/6-311+G** calculated structural parameters for the *ee*, *ea*, and *aa* configurations of compounds **1–4**

	1			**2**			**3**			**4**		
Compound State	*aa*	*ea*	*ee*	*aa*	*ea*	*ee*	*aa*	*ea*	*ee*	*aa*	*ea*	*ee*
Bond lengths (Å)												
$r_{1\text{-}2}$	1.465	1.448	1.456	1.878	1.875	1.872	2.001	1.997	1.995	1.548	1.534	1.538
$r_{2\text{-}3}$	1.465	1.472	1.456	1.878	1.871	1.872	2.001	1.994	1.995	1.548	1.540	1.538
$r_{3\text{-}4}$	1.467	1.464	1.461	1.873	1.870	1.874	2.003	2.000	2.003	1.544	1.539	1.538
$r_{4\text{-}5}$	1.541	1.532	1.528	1.536	1.538	1.539	1.532	1.535	1.536	1.536	1.534	1.534
$r_{5\text{-}6}$	1.541	1.538	1.528	1.536	1.538	1.539	1.532	1.535	1.536	1.536	1.536	1.534
$r_{6\text{-}1}$	1.466	1.467	1.461	1.873	1.875	1.874	2.003	2.005	2.003	1.544	1.534	1.538
Bond angles (°)												
$\theta_{1\text{-}2\text{-}3}$	117.7	113.5	111.8	125.7	116.75	110.1	125.2	116.3	109.3	116.6	113.0	113.2
$\theta_{2\text{-}3\text{-}4}$	110.5	110.3	111.2	101.5	98.2	97.9	101.1	96.3	95.8	110.2	110.2	110.3
$\theta_{3\text{-}4\text{-}5}$	113.1	110.5	110.1	118.7	112.3	113.1	118.9	113.2	114.0	112.8	112.2	112.1
$\theta_{4\text{-}5\text{-}6}$	109.1	109.9	110.3	113.9	113.7	113.5	114.6	114.5	114.3	110.0	111.4	111.6
$\theta_{5\text{-}6\text{-}1}$	113.1	112.9	110.1	118.7	119.5	113.2	118.9	119.9	114.0	112.8	112.9	112.1
$\theta_{6\text{-}1\text{-}2}$	110.5	110.3	111.2	101.5	100.6	97.9	101.1	119.9	95.8	110.2	109.0	110.3
Torsion angels (°)												
$\phi_{1\text{-}2\text{-}3\text{-}4}$	52.1	60.4	59.2	31.2	58.0	64.4	23.4	56.2	64.1	48.6	54.0	54.6
$\phi_{2\text{-}3\text{-}4\text{-}5}$	−51.7	−57.1	−56.4	−44.6	−64.6	−62.0	−42.3	−65.4	−62.9	−51.5	−54.0	−53.0
$\phi_{3\text{-}4\text{-}5\text{-}6}$	52.9	52.9	54.0	65.7	69.7	66.9	69.6	73.2	69.4	56.7	55.1	54.7
$\phi_{4\text{-}5\text{-}6\text{-}1}$	−52.9	−51.2	−54.0	−65.7	−59.9	−66.9	−69.7	−62.5	−69.4	−56.7	−54.5	−54.7
$\phi_{5\text{-}6\text{-}1\text{-}2}$	51.7	52.8	56.4	44.5	45.8	62.0	42.3	45.8	62.8	51.5	52.6	53.0
$\phi_{6\text{-}1\text{-}2\text{-}3}$	−52.1	−57.3	−59.2	−31.2	−49.0	−64.4	−23.4	−47.7	−64.1	−48.6	−53.0	−54.6

$LP_{eq}M1 \rightarrow \sigma^*_{C2\text{-}M3}$ electronic delocalizations in the *ea* configurations of compound **1** (see Tables 2 and 3).

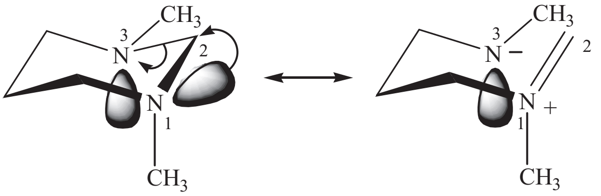

Scheme 2 Schematic representation of electron delocalization (from $LP_{eq}M1$ to $\sigma^*_{C2\text{-}M3}$) in the *ea* configuration of compound **1**.

Surprisingly, contrary to the observed results for the $\sigma_{M1\text{-}C2}$ and $\sigma_{C2\text{-}M3}$ bond lengths of the *ea* configurations of compound **1**, the results revealed a reverse trend for the *ea* configurations of compounds **2** and **3**. B3LYP/6-311+G** results showed that the $\sigma_{M1\text{-}C2}$ and $\sigma_{C2\text{-}M3}$ bond lengths in the *ea* configurations of compounds **2** and **3** are 1.875, 1.871 and 1.997, 1.994 Å, respectively (see Table 6). Since the stabilization (resonance) energy associated with $LP_{eq}M1 \rightarrow \sigma^*_{C2\text{-}M3}$ electronic delocalizations in the *ea* configurations of **2** and **3** are smaller than those in compound **1** (the GAE decrease notably for the higher row substituents), it seems that the 1,3-syn-axial repulsions could play an important role in the lengthening of $\sigma_{M1\text{-}C2}$ bonds of compounds **2** and **3**, compared to their $\sigma_{C2\text{-}M3}$ bonds (see Scheme 3).

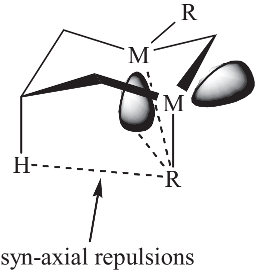

Scheme 3 Schematic representation of 1,3-syn-axial-repulsion in the *ea* configurations of compounds **1–3**.

CONCLUSION

The above reported DFT calculations and NBO analysis provided a reasonable picture from structural, energetic, bonding, and stereoelectronic points of view for the configurational preference in compounds **1**–**3**. Effectively, based on the calculated Gibbs free-energy (GFE) values, the *ea* configurations of compounds **1–3** are more stable than their *ea* and *ee* configurations and the energy differences between the *ee-ea*, *ee-aa*, and *ea-aa* configurations decrease from compound **1** to compound **3**. Also, the smaller energy differences between the *ee-ea*, *ee-aa*, and *ea-aa* configurations of compounds **1–3**, compared to compound **4**, is a result of the impact of the GAE on the various configurations of compounds **1–3**.

In addition, NBO results revealed also that the stabilization energies associated with $LP_{eq}M1 \rightarrow \sigma^*_{C2\text{-}M3}$ electronic delocalizations decrease from the *ea* and *aa* configurations of compound **1** to compound **3**. Also, the increase of the $LP_{eq}M1$ nonbonding orbital occupancies and also the decrease of the $\sigma^*_{C2\text{-}M3}$ antibonding orbital occupancies in the *ea* and *aa* configurations of compounds **1–3** could be justified by the decrease of the $LP_{eq}M1 \rightarrow \sigma^*_{C2\text{-}M3}$ electronic delocalizations from the *ea* and *aa* configurations of compound **1** to compound **3**. The contribution of the GAE in the stability of the *ea* and *aa* configurations of compounds **1–3** could be controlled by the off-diagonal [or orbital overlap (S)] factor.

The rationalization of the configuration preference solely in terms of dipole–dipole interactions fails to account qualitatively for the *ee* preferences in compounds **1–3**, but the variations of the differences of the dipole moments between the *ee-ea* configurations reasonably explains the decrease of the energy differences between the *ee* and *ea* configurations from compound **1** to compound **3**.

Also, the $\sigma_{M1\text{-}C2}$ bond length in the *ea* configurations of compound **1** is significantly contracted in comparison to their $\sigma_{C2\text{-}M3}$ bonds. Contrary to compound **1**, the $\sigma_{C2\text{-}M3}$ bond lengths of the *ea* configurations of compounds **2** and **3** are longer than their $\sigma_{M1\&bond;C2}$ bonds, which could be the result of the 1,3-syn-axial repulsions.

REFERENCES

1. Westheimer, F. H. In: M. S. Neman (Ed.), *Steric Effects in Organic Chemistry*; John Wiley & Sons, Inc., New York: **1956**.
2. Hendrickson, J. B. *J. Am. Chem. Soc.* **1967**, *89*, 7036.
3. Riddell, F. G.; Williams, D. A. R. *Tetrahedron Lett.* **1971**, *23*, 2073.
4. Jones, R. A. Y.; Katritzky, A. R.; Snarey, M. *J. Chem. Soc. (B)* **1970**, 131.
5. Eliel, E. L.; Kopp, L. D.; Dennis, J. E.; Evans Jr., S. A. *Tetrahedron Lett.* **1971**, *37*, 3409.
6. Hutchins, R. O.; Kopp, L. D.; Eliel, E. L. *J. Am. Chem. Soc.* **1968**, *90*, 7174.
7. Eliel, E. L. *Angew. Chem., Int. Ed. Engl.* **1972**, *11*, 739.
8. Carballeira, L.; Pérez-Juste, I. *J. Comput. Chem.* **2000**, *21*, 462.
9. Carballeira, L.; Pérez-Juste, I. *J. Phys. Chem. A* **2000**, *104*, 9362.
10. Eskandari, K.; Vila, A.; Mosquera, R. A. *J. Phys. Chem. A* **2007**, *111*, 8491.
11. Schleyer, P. v. R.; Jemmis, J. E.; Spitznagel, G. W. *J. Am. Chem. Soc.* **1985**, *107*, 6393.
12. Knuppel, P. C.; Pawelke, G.; Sommer, H.; Stelzer, O.; Oberhammer, H.; Lappert, M. F.; Suffolk, R. J.; Watts, J. D. *J. Organom. Chem.* **1988**, *355*, 55.
13. Frisch, M. J. et al., GAUSSIAN 98 (Revision A.3); Gaussian, Inc. Pittsburgh, PA: **1998**.
14. Becke, A. D. *J. Chem. Phys.* **1993**, *98*, 5648.
15. Lee, C.; Yang, W.; Parr, R. G. *Phys. Rev. B* **1988**, *37*, 785.
16. Vosko, S. H.; Wilk, L.; Nusair, M. *Can. J. Phys.* **1980**, *58*, 1200.
17. Stephens, P. J.; Devlin, F. J.; Chabalowski, C. F.; Frisch, M. J. *J. Phys. Chem.* **1994**, *98*, 11623.
18. Seminario, J. M.; Politzer, P. (Eds.), *Modern Density Function Theory, A Tool for Chemistry*; Elsevier, Amsterdam: **1995**.
19. Reed, A. E.; Weinstock, R. B.; Weinhold, F. *J. Chem. Phys.* **1985**, *83*, 735.
20. Reed, A. E.; Curtiss, L. A.; Weinhold, F. *Chem. Rev.* **1988**, *88*, 899.
21. Foster, J. P.; Weinhold, F. *J. Am. Chem. Soc.* **1980**, *102*, 721.
22. Brunck, T. K.; Weinhold, F. *J. Am. Chem. Soc.* **1978**, *101*, 1700.
23. Reed, A. E.; Weinhold, F. *J. Chem. Phys.* **1985**, *83*, 1736.
24. Reed, A. E.; Schleyer, P. v. R. *J. Am. Chem. Soc.* **1987**, *109*, 7362.
25. Nori-Shargh, D.; Deyhimi, F.; Boggs, J. E.; Jameh-Bozorghi, S.; Shakibazadeh, R. *J. Phys. Org. Chem.* **2007**, *20*, 355.

26. Nori-Shargh, D.; Yahyaei, H. *J. Mol. Struct. THEOCHEM* **2009**, *913*, 8.
27. Nori-Shargh, D.; Hassanzadeh, N.; Kosari, M.; Sharifi, S. *J. Mol. Struct. THEOCHEM* **2010**, *940*, 129.
28. Nori-Shargh, D.; Yahyaei, H.; Boggs, J. E. *J. Mol. Graphics Modell.* **2010**, *28*, 807.
29. Glendening, E. D.; Badenhoop, J. K.; Reed, A. E.; Carpenter, J. E.; Bohmann, J. A.; Morales, C. M.; Weinhold, F. NBO Version 5.G; Theoretical Chemistry Institute, University of Wisconsin, Madison, WI: **2004**.
30. Dionne, P.; St-Jacques, M. *J. Am. Chem. Soc.* **1987**, *109*, 2616.
31. Wiberg, K. B.; Murcko, M. A. *J. Phys. Chem.* **1987**, *91*, 3616.